sustainability

MDPI

Article

Mangrove Vertical Soil Accretion and Potential Risk—Resilience Assessment of Sea-Level Rise in the Beilun Estuary and Guangxi Coastal Zone, China

Juan Zhang [1,2,†], Zhongchen Jiang [1,3,†], Dongmei Li [1,3,4,†] and Peng Zhou [1,3,4,*]

[1] Nansha Islands Coral Reef Ecosystem National Observation and Research Station & Key Laboratory of Marine Environmental Survey Technology and Application, Ministry of Natural Resources (MNR), Guangzhou 510300, China; zj345278144@foxmail.com (J.Z.); jcc1967@163.com (Z.J.); lidmay@foxmail.com (D.L.)
[2] South China Sea Marine Forecast and Hazard Mitigation Center, Ministry of Natural Resources (MNR), Guangzhou 510310, China
[3] South China Sea Ecological Center, Ministry of Natural Resources (MNR), Guangzhou 510300, China
[4] Key Laboratory of Global Change and Marine-Atmospheric Chemistry, Ministry of Natural Resources (MNR), Xiamen 361005, China
* Correspondence: samzhou2@126.com; Tel.: +86-20-89111586; Fax: +86-20-84457983
† These authors contributed equally to this work.

Abstract

Mangrove ecosystems play a critical role in climate regulation, carbon sequestration, and pollution mitigation. However, their long-term resilience to accelerating sea-level rise (SLR) under global climate change scenarios remains uncertain. Vertical soil accretion is a critical factor in determining the vulnerability of mangrove wetlands to SLR. In this study, vertical soil accretion rates in a mangrove wetland in the Beilun estuary were measured using a ^{210}Pbex dating method. Based on recently acquired data and previously available data, we conducted the first systematic assessment of SLR risk in mangrove wetlands in the Guangxi coastal zone in the context of increasing global climate change and extreme weather. The results show that the vertical soil accretion rate of 6.72 ± 1.91 (4.22–10.54) mm/a in the Beilun estuary is slightly higher than SLR rate in the Guangxi coastal zone. Concurrently, our results indicate that mangroves with thriving root systems enhance soil accretion through biotic controls in the Beilun estuary, while significant changes in soil sources and hydrodynamic forces during the 1980s and 2000s contributed to adaptation to SLR. Additionally, by linking sedimentation dynamics with SLR projections, we reveal that current accretion rates in some mangrove areas in the Guangxi coastal zone are insufficient to offset the projected SLR by the end of 2050 and 2100. This finding offers a new perspective on the traditional assumption of inherent resilience in mangroves while revealing the adaptive capacity of mangroves in the Beilun estuary and Guangxi coastal zone under projected SLR scenarios. It underscores the need for integrated management strategies that balance sediment supply maintenance and ecological restoration, which are critical to ensuring the long-term resilience of mangrove ecosystems, in line with sustainability principles.

Keywords: mangrove wetlands; vertical soil accretion; sea-level rise; potential risk and resilience assessment; the Beilun estuary and Guangxi coastal zone

check for updates

Academic Editor: Teodor Rusu

Received: 28 June 2025
Revised: 3 September 2025
Accepted: 4 September 2025
Published: 9 September 2025

Citation: Zhang, J.; Jiang, Z.; Li, D.; Zhou, P. Mangrove Vertical Soil Accretion and Potential Risk—Resilience Assessment of Sea-Level Rise in the Beilun Estuary and Guangxi Coastal Zone, China. *Sustainability* **2025**, *17*, 8099. https://doi.org/10.3390/su17188099

Copyright: © 2025 by the authors. Licensee MDPI, Basel, Switzerland. This article is an open access article distributed under the terms and conditions of the Creative Commons Attribution (CC BY) license (https://creativecommons.org/licenses/by/4.0/).

1. Introduction

Mangroves are unique woody plants found on tropical and subtropical coastlines that possess both terrestrial and marine properties. They provide an important habitat for a variety of species, supplying nursery and/or breeding, feeding, and sheltering environments [1–3]. Mangroves have significant ecological functions, absorbing waves and tides, safeguarding shores and farmlands [4,5], preserving biodiversity [3,6], hastening pollutant degradation, and promoting tourism and education [7–11]. Global climate warming causes sea level rise (SLR) due to the melting of polar glaciers and the thermal expansion of upper sea water. According to the WMO (2020) [12], the global average SLR accelerated by 3.3 $\pm$ 0.3 mm/a during the period between 1993 to 2020, reaching the highest peak in satellite observation records. Accelerated SLR, intensified extreme marine events, and human activities have caused coastal erosion, reduced natural coastlines, and threatened coastal ecosystems. Coastal wetlands are highly vulnerable to SLR, which results in significant decreases in coastal wetland area and biodiversity and habitat degradation [13,14]. Over the last century, almost half of the world's coastal wetlands have disappeared. If greenhouse gas emissions continue without reduction, under the RCP 8.5 scenario, up to 90% of existing coastal wetlands worldwide will be degraded by 2100, leading to frequent extreme sea level events, possibly even annually [15].

The relative SLR rate in tropical and subtropical locations is projected to increase from the current rate of ~3.4 mm/a to a mean estimate of ~5 mm/a (1.47 times the current rate) under low-emissions scenarios and ~10 mm/a (2.94 times the current rate) under high-emissions scenarios by 2100 [16,17]. If the relative SLR rate surpasses 6.1 mm/a (the threshold), mangroves will not be able to maintain sustained growth (>90% probability) [17]. This alarming trend is exacerbated by an accelerating SLR and diminishing sediment supply. SLR impacts on coastal wetland ecosystems due to global climate change and its mutual feedback processes and mechanisms have received increasing attention from the international scientific community. If SLR rate exceeds the rate of vertical soil accretion, mangrove wetlands may be gradually submerged. As a result, mangroves will migrate to land to avoid inundation [1,18–20].

The combined promotion of mangrove protection and SLR mitigation lies at the core of sustainable development. Environmentally, mangroves provide a natural barrier against SLR. Economically, healthy mangroves boost fisheries and ecotourism. Socially, they safeguard coastal livelihoods and cultural heritage and encourage participation in community governance, enhancing social cohesion. SLR is a significant driving force for the landward migration of mangroves. Overlying mangrove plants can reduce SLR rate by trapping sediment [21–27]. However, their ability to adapt to SLR remains a topic of interest. For approximately 69% of mangrove surface elevation sites in the Indo-Pacific region, the current SLR rate exceeds the gain in soil surface elevation, which could result in submersion as early as 2070 [19]. The material accumulation of soil pools in coastal wetlands (especially vertical soil accretion) is an important form of natural capital that plays a role in regulating the elevation change in coastal wetlands and resisting SLR. Vertical soil accretion is a crucial factor in determining the vulnerability of mangrove wetlands to SLR risk. Recent assessments [15] indicate significant declines due to anthropogenic pressures, highlighting the urgent need to quantify mangrove vulnerability to SLR.

The total mangrove area in China increased from 25,829 hectares [28] to 30,300 hectares by the end of 2024. The total mangrove area in the Guangxi coastal zone reached 10,600 hectares, contributing 35% of China's total mangrove area. The Beilun Estuary National Mangrove Forest Reserve Region (BENMFRR) covers 3300 hectares and is located in the southern offshore area of Fangchenggang city (including Gangkou district and Dongxing city) [29–32]. The BENMFRR is a tidal flat wetland located on the northwestern

coast of the Beibu Gulf and and straddled the eastern section of the China-Vietnam border. It is fed by three rivers of the Beilun estuary, Jiangping estuary, and Pearl Bay [29,33]. The main issues in this area are habitat fragmentation and loss [34] and pollution [35–37]. Recent years have seen an increase in the invasion of non-native species, pests, and diseases [29,30,32,38], as well as pollution with microplastics and man-made debris [33,39,40]. Despite these problems, there have been few studies conducted on SLR risk in mangrove wetlands, specifically in relation to vertical soil accretion.

The accretion profile of vertical soil cores in wetlands is rich in environmental information. It is also an important tool for tracing global historical change and predicting the impact of future climate change on wetlands. From the perspective of isotope oceanography, radionuclides are unique tracers of vertical soil accretion processes due to their accurate and reliable time-scale advantages. Given that climate change—both past and present—results in changes in mangrove wetland soils (sources, composition, and rates of deposition) on both spatial and temporal scales, these radionuclides play a key role in studying the non-steady-state sediment dynamics of coastal wetlands. Hence, carefully attributing and using these isotope data could be very important. It is important to strengthen our investigation into the current status of the soil matrix layer in coastal wetlands to explore the characteristics of changes in vertical soil accretion processes and their regulatory mechanisms over the decadal time-scale using the radiometric $^{210}Pb_{ex}$ dating method [27,41].

In this study, we collected four soil core samples from the Shijiao and Rongshutou transects in the Beilun estuary mangrove ecosystem on 9 June 2020 to study the effects of historical change. The samples underwent analysis for ^{238}U, ^{226}Ra, ^{210}Pb, ^{228}Th, ^{228}Ra, ^{40}K, and ^{137}Cs using HPGe γ spectrometry. Accretion rates were calculated using $^{210}Pbex$ ($T_{1/2}$ = 22.3 a) and ^{137}Cs ($T_{1/2}$ = 30.2 a) dating methods. Previous studies primarily focused on sedimentation patterns in deltaic regions (e.g., Xia et al., 2015) [27], but the response mechanisms of estuarine mangroves in the Beilun estuary remain poorly understood. Whether mangrove vertical soil accretion will sufficiently counteract SLR rate in the future is a critical question addressed in this study, in which we conduct the first systematic assessment of SLR risk to mangrove wetlands in the Guangxi coastal zone based on our recently obtained data and previously available data. We carried out this work by integrating radiometric dating and hydrodynamic modeling. Our findings provide critical insights into the mangrove adaptive capacity of the Beilun estuary and Guangxi coastal zone under projected SLR scenarios, underscoring the need for integrated management strategies that balance sediment supply maintenance and ecological restoration to ensure long-term resilience.

The aim is to develop a fundamental understanding of the relationship between mangrove health, human activity, and coastal environmental changes. First, the profiles of radionuclides are interpreted in order to determine a decadal average accretion rate (10–99 a) with historical event horizons and to investigate how mangroves respond to SLR. Second, radiometric ^{210}Pb data are co-located with SLR records in close proximity to determine tidal wetland stability. It is important to quantify the trajectory of future vertical changes in coastal wetland soils to provide an isotopic tool to study the conservation and restoration of coastal wetlands. This radiometric technique may be applicable to the burial/sequestration rates of atmospheric CO_2 and organic carbon in wetland soils. These results can aid policy decisions and provide assurance for carbon market investments. Additionally, our results may encourage the protection of mangrove wetlands and support their sustainable utilization.

2. Methodology

2.1. Sampling

Four soil cores were collected from the Shijiao (SJ) transect (two stations: SJ-1 and SJ-2) and Rongshutou (RST) transect (two stations: RST-1 and RST-2) on 9 June 2020 (Figure 1), using a PVC pipe with a diameter of 90 mm. The cores were transported to the laboratory and immediately sub-sampled at intervals of either 3.0 or 5.0 cm. After air-drying, the sub-samples were subjected to biodetritus removal, ground, and homogeneously mixed for the analysis of gamma radionuclides.

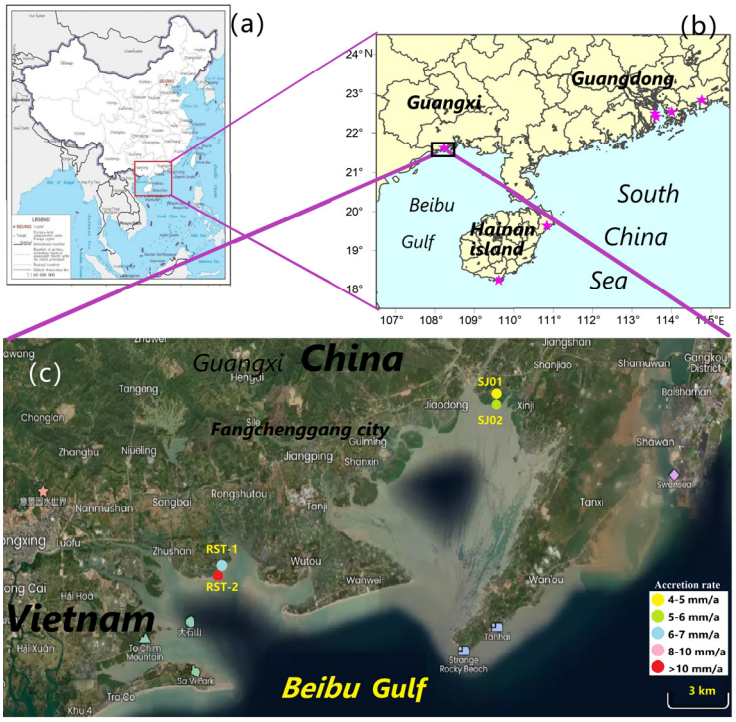

Figure 1. (**a**–**c**) Transects and stations for debris monitoring in the Beilun estuary mangrove forest region.

2.2. Measurement of Gamma Radionuclides

After sifting and compaction, the sub-samples were packed into boxes and sealed for over 20 days to achieve secular equilibrium of ^{226}Ra and ^{222}Rn [42–44]. Gamma-ray spectrometry (BE5030, Canberra, Australia) in an energy range of 3 keV–3 MeV was employed to measure the activity of radionuclides (^{40}K, ^{210}Pb, ^{226}Ra, ^{228}Ra, ^{228}Th, ^{238}U, and ^{137}Cs) in 24-hour counts, following equilibrium correction (^{226}Ra-^{222}Rn secular equilibrium achieved after 20 days of sample equilibration). Details of measurement using gamma-ray energy peaks can be found in References [44,45]. The HPGe-γ spectrometer was calibrated regularly (National Institute of Metrology China, Beijing, China). The efficiency calibration used passive efficiency software. The detection and verification used an S/N: 13,000,566 point source and a GBW08304a standard (river mud). The accretion rate using the Constant Initial Concentration model (CIC or CA) [46,47] instead of the sedimentary rate to accurately estimate the soil accumulation rate and to reconstruct the chronology of the soil cores. ^{137}Cs and ^{210}Pb were analyzed simultaneously [42–44] for supplementary data, verification, and correction with two sets of data. Some historical event horizons of significant storm surges were used to verify the ^{210}Pbex dating method used in this study.

3. Results

The specific activities of the gamma radionuclides are shown in Figure 2 and Tables S1 and S2. The specific activities of ^{40}K, ^{210}Pb, ^{226}Ra, ^{228}Ra, ^{228}Th, ^{238}U, and ^{137}Cs in the SJ-1 core were 138.8 ± 6.1 (119–177), 48.4 ± 7.7 (23.4–96.8), 18.2 ± 0.5 (15.6–21.4), 25.4 ± 0.9 (21.8–29.8), 24.1 ± 0.8 (21.1–28.6), 52.1 ± 3.0 (32.3–63.0), and 0.51 ± 0.08 (<0.19–0.67) Bq/kg, respectively. The specific activities of ^{40}K, ^{210}Pb, ^{226}Ra, ^{228}Ra, ^{228}Th, ^{238}U, and ^{137}Cs in the SJ-2 core were 133 ± 6 (105–176), 55.8 ± 9.0 (23.5–98.6), 17.6 ± 0.6 (15.4–21.5), 25.2 ± 1.1 (22.5–26.9), 23.3 ± 1.2 (21.1–25.6), 56.2 ± 4.5 (46.2–68.9), and 0.47 ± 0.12 (<0.18–0.55), respectively. In the RST-1 core, the specific activities of ^{40}K, ^{210}Pb, ^{226}Ra, ^{228}Ra, ^{228}Th, ^{238}U, and ^{137}Cs were 82.4 ± 4.0 (59.6–114), 68.9 ± 10.4 (46.8–82.9), 21.9 ± 0.8 (19.3–24.7), 27.8 ± 1.2 (23.4–31.2), 28.2 ± 1.4 (24.1–32.3), 64.4 ± 5.1 (46.8–83.7), and <0.39 Bq/kg, respectively. In the RST-2 core, the specific activities of ^{40}K, ^{210}Pb, ^{226}Ra, ^{228}Ra, ^{228}Th, ^{238}U, and ^{137}Cs were 105 ± 4.9 (74.2–150), 56.4 ± 9.0 (38.8–87.0), 22.4 ± 0.8 (17.2–31.4), 26.4 ± 1.2 (21.7–34.0), 25.7 ± 1.3 (20.9–33.1), 65.6 ± 4.9 (45.7–107), and <0.69 Bq/kg, respectively.

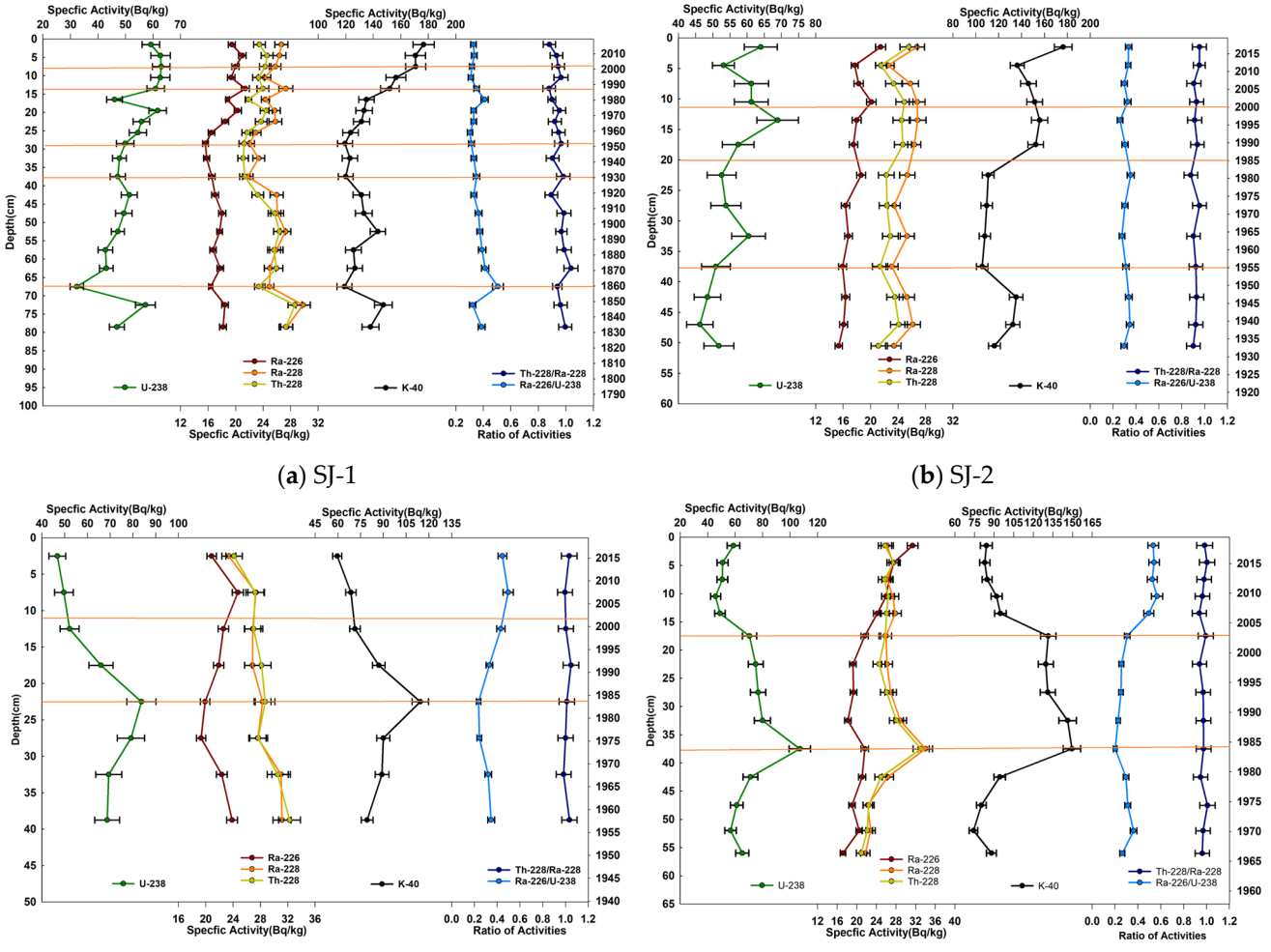

(**a**) SJ-1 (**b**) SJ-2

(**c**) RST-1 (**d**) RST-2

Figure 2. Distribution of ^{40}K, ^{226}Ra, ^{228}Ra, ^{228}Th, ^{238}U and ratios of ^{228}Th/^{228}Ra and ^{226}Ra/^{238}U in the cores (**a**) SJ-1, (**b**) SJ-2, (**c**)RST-1, and (**d**) RST-2.

The profiles of ^{210}Pb, ^{226}Ra, and ^{210}Pb$_{ex}$ are shown in Tables S3–S5. When calculating the accretion rate, it is important to exclude ^{210}Pbex data from the surface, where the values are is generally lower than in the subsurface. After discarding abnormalities

present from the surface and bottom sediment, the accretion rates were determined using the ^{210}Pbex dating method. It was not possible to use ^{137}Cs for dating and verifying the ^{210}Pbex dating results because its specific activity was less than the minimum detectable activity. At stations SJ-1, SJ-2, RST-1, and RST-2, the accretion rates were 4.223, 5.843, 6.279, and 10.537 (6.72 ± 1.91) mm/a, respectively; the ratios of ^{228}Th/^{228}Ra were 0.95 ± 0.05 (0.88–1.04), 0.92 ± 0.06 (0.88–0.96), 1.01 ± 0.07 (0.98–1.05), and 0.97 ± 0.06 (0.94–1.01), respectively; and the ratios of ^{226}Ra/^{238}U were 0.35 ± 0.02 (0.30–0.51), 0.31 ± 0.03 (0.26–0.35), 0.36 ± 0.03 (0.24–0.50), and 0.37 ± 0.03 (0.20–0.57), respectively. ^{228}Ra and ^{228}Th are close to equilibrium, but ^{238}U and ^{226}Ra are in disequilibrium.

4. Discussion

4.1. Mangrove Soil Accretion Rates

4.1.1. Profiles of the $^{210}Pb_{ex}$ in the Soils Cores and Verification of Historical Event Horizons

In three cores, SJ-1, SJ-2, and RST-1 (Figure S1), abnormal $^{210}Pb_{ex}$ data from topsoil soil (≤15 cm) could not be used to calculate dates due to physical and/or biological disruptions and the redistribution of radionuclides. Physical disturbances, such as hydrodynamic and storm surge activities, can induce the re-suspension and re-deposition of suspended particles at the water–sediment interface, disrupting the closed equilibrium state of the surface sediment and impeding sedimentation. However, sediments following the water–sediment interface remain closed. Biological disturbances, such as crab burrowing, cause sediment mixing at the water–sediment interface but typically do not disrupt sedimentary interface stability. Physical or biological disturbances can alter anticipated stratigraphy.

It is difficult to explain the generally lower ^{210}Pb specificity of the tidal flat surface compared to the subsurface features by the above-described periodic fluctuations alone. Radionuclides between the deposition and redox interfaces could be redistributed within the sediment–interstitial water system due to significant tidal flat water and groundwater table level fluctuations. The redistribution of radionuclides can amplify, resulting in a significant difference between the relatively lower surface layer values and the maximum value near the redox interface in the subsurface layer. The stable initial concentration of particulate radionuclides, such as ^{234}Th and ^{238}U, cannot be established until redistribution is complete [48,49].

Thus, Goldberg's dating model may not be applicable in unstable wetland, marsh, and intertidal zone environments. This is because the ^{210}Pbex dating method relies on two assumptions: a stable ^{210}Pb supply source and an undisturbed closed system after deposition. The dilution of ^{210}Pb reaching the sediment surface is caused by various factors, including waves, tides/tidal currents, storms, and human activity. In addition, sediment sources often change, storm events cause erosion and deposition, surface sediments are mixed, and horizontal transportation can occur.

4.1.2. Vertical Soil Accretion Rates in the Guangxi Mangrove Wetland

Figure 3 depicts the vertical soil accretion rates in mangrove wetlands situated the Guangxi coastal zone (Table S6) [27,41,50–53]. It can be observed that the vertical soil accretion rates in the Beilun estuary mangrove wetland (4.223–10.537 mm/a, 6.72 mm/a, n = 4) determined in our study are comparable to those in the Pearl Bay (6.7 mm/a) [54,55]. Additionally, our study, along with previous publications [50,54,55], indicates a regional accretion in the mangrove wetlands of Fangchenggang city, with an accretion rate of 1.10–10.54 (4.90 ± 1.95 mm/a, n = 10) mm/a over the past decades.

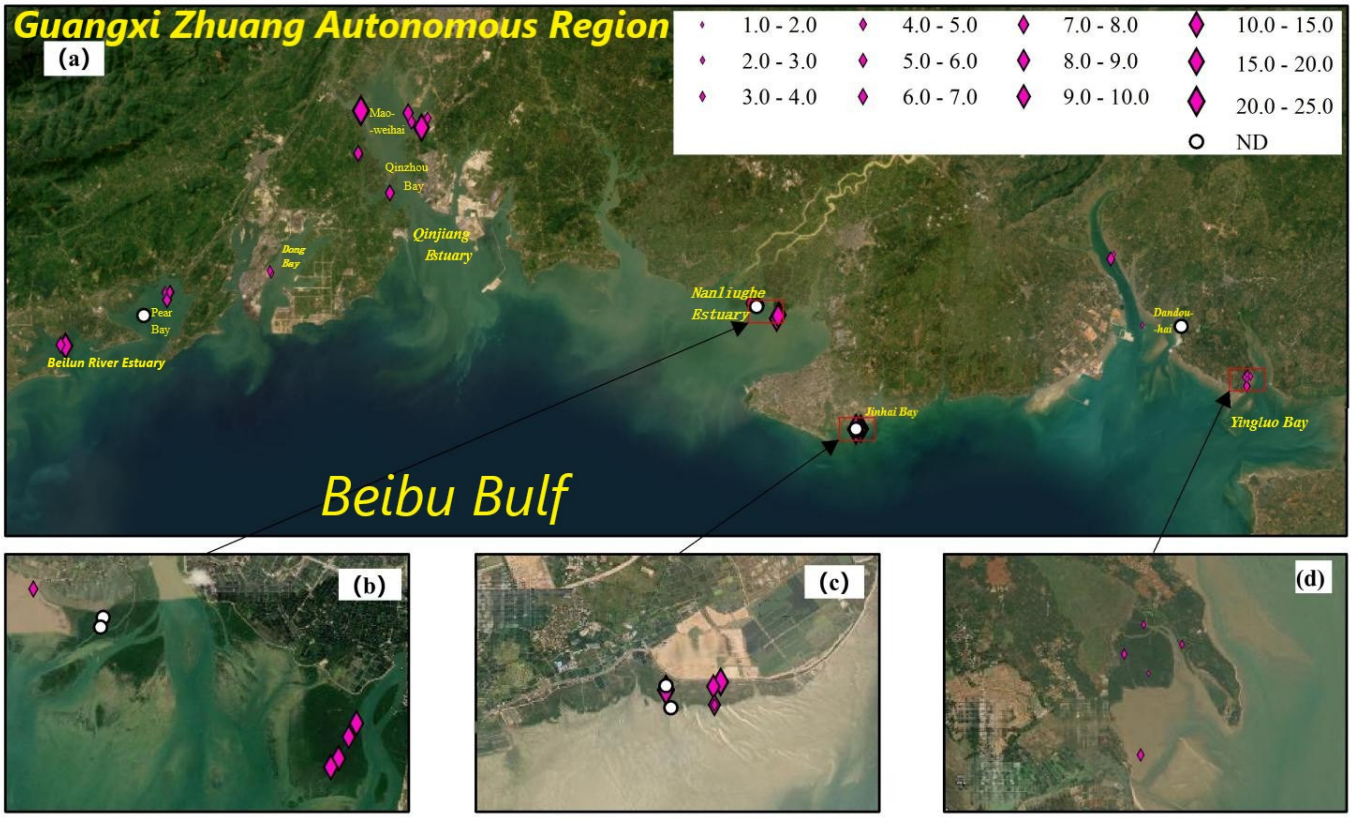

Figure 3. Vertical soil accretion rates of mangrove wetland in Fangchenggang city and the Guangxi coastal zone. (**a**) Guangxi coast zone, (**b**) Muanjing, Nanliughe estuary in Beihai, (**c**) Jinhai Bay (Daguansha) in Beihai, (**d**) Yingluo bay in Beihai. (ND stands for no accretion rate data).

Our study and others [27,41,50–55] published in recent decades indicate that the Guangxi coastal zone has an accretion rate of 1.1–26 (7.17 ± 4.15, n = 37) mm/a. Our results are comparable to those attained in the Maoweihai–Qinjiang estuary (in Qingzhou city), Yingluo Bay (in Beihai city), Dandouhai (in Beihai city), the Nanliughe estuary (in Beihai city), and Daguansha (i.e., Jinhai Bay) (in Beihai city).

4.2. Implications of Sediment Supply to Mangrove Wetlands

4.2.1. Influence of Tidal Level on Soil Accretion Rate

In the Beilun estuary, the soil accretion rates are higher at low-tide and medium-tide stations than at the high–medium-tide station. The results are consistent with those found in the Jiulongjiang estuary [56,57], suggesting that the particulate matter suspended in wetlands originates primarily from upstream river inputs rather than from the erosion of surrounding coastlines. This is attributed to the protective nature of mangroves, which shield the shore/farmland. Mangroves' dense root systems reduce wave and current impacts to weaken erosive forces on shorelines and farmland, while their intricate roots and branches trap sediment to promote deposition and maintain coastal stability. The soil accretion rate of mangrove wetlands impacts tidal levels, with higher rates at low- and medium-tide stations than at high–medium-tide stations. This disparity stems from multiple factors. Sediment supply plays a key role; low- and medium-tide zones, which are closer to river estuaries or other sources, receive more sediment, facilitating greater accumulation. Hydrodynamic conditions also matter. In low- and medium-tide areas, moderate water flow allows for sediment deposition, while stronger currents in high–medium- tide zones hinder it. Mangrove vegetation differs across zones: more robust growth in low- and medium-tide areas enables better sediment interception by roots,

whereas mangroves in high–medium-tide areas are exposed to harsher tides, making them less effective. Finally, topography impacts accumulation. Low- and medium-tide regions often have features, like shoals, that favor sediment accumulation, while high–medium-tide areas with a flatter terrain allow sediment to be carried away easily.

If the accretion rate at the high–medium-tide station exceeds the rate at the low- or medium-tide stations, it is probable that serious coastal erosion or soil loss is taking place around the mangrove wetland area. There may also be other causes, such as changes in the local hydrographic regime (abnormal changes in river runoff, tidal patterns, etc.), human activity, or ecological changes in the mangrove wetland itself (such as mangrove degradation, which weakens its sediment-trapping function; in some cases, specific changes may lead to abnormal sediment distribution).

4.2.2. Profiles of Gamma Radionuclides and Verification of Historical Event Horizon

Distinct peaks (inflection points) of ^{238}U, ^{226}Ra, ^{228}Ra, ^{228}Th, and ^{40}K in the 1980s (1980–1990) were observed in the cores of SJ-1and SJ-2 (Figure 2a,b). These findings provide important insights into the impact of sediment supply on mangrove wetlands over time. Subtle yet unmistakable peaks in the 1950s (1950–1960) and the 2000s (2000–2005) were also observed. The ratios of ^{228}Th/^{228}Ra and ^{226}Ra/^{238}U exhibited slight inflection points in the 2000s (2000–2005) and the 1980s (1980–1990).

In the RST-1 and RST-2 cores (Figure 2c,d), distinct peaks of ^{238}U, ^{226}Ra, ^{228}Ra, ^{228}Th, and ^{40}K in the 1980s (1980–1990) were observed. Similar peaks in the 2000s (2000–2005) were also observed. For the ratios of ^{228}Th/^{228}Ra and ^{226}Ra/^{238}U, subtle yet distinct peaks in 1980–1990 and 2000–2005 were observed. The vertical profiles from the 1980s (1980–1990) and the 2000s (2000–2005) are in accordance with the huge storm surges of No. 8609-Sarah, in 1986 and No. 0312-Krovanh, in 2003, respectively. Historical event horizons are of great importance in the sedimentary dating of wetland soils and tidal flats [5,58]. For example, the impact of huge storm surges on these areas has been studied [41,51]. Thus, verifying the rationality of our ^{210}Pbex dating results for mangrove wetlands in the Beilun estuary has been crucial in determining the historical event horizon of massive storm surges in this area.

4.2.3. Changes in Sediment Supply to the Beilun Estuary Mangroves over Previous Decades

Sufficient sediment, which mainly comprises mud, sand, and organic matter, is a crucial indication of the health of mangrove wetlands. The radionuclide profiles demonstrate that sediment input into the Beilun estuary has changed significantly in recent decades. However, the wetland's sediment supply remains sufficient to offset SLR. The similar vertical profiles of various radionuclides and their ratios (^{40}K, ^{226}Ra, ^{228}Ra, ^{228}Th, and ^{238}U and the ratios of ^{228}Th/^{228}Ra and ^{226}Ra/^{238}U) in the 1980s and the 2000s provide evidence of significant changes in the source of vertical soil accretion and hydrodynamic forces in the Beilun estuary mangrove wetland.

The distinct peaks in the 1980s may have resulted from intensified human activity, which included unreasonable land development and the destruction of the mangrove ecosystem. The coastal wetland's material and energy equilibrium was disrupted by unregulated reclamation, aquaculture, and other damaging coastal practices. The subtle but noticeable peaks observed for the 2000s were influenced by an increase in awareness and concern for environmental issues at the early 21st century, along with subsequent implementation of diverse environmental protection measures. The observed shifts in the ^{228}Th/^{228}Ra and ^{226}Ra/^{238}U ratios in 2000–2005 suggest changes in sediment provenance, likely due to enhanced terrigenous input following hydrological regulation projects in the Beilun River catchment [59]. The Beilun estuary mangrove wetland was established as a provincial

marine reserve in 1990 and subsequently promoted to National Nature Reserve status. In 2008, it was included in the List of International Important Wetlands and subsequently became one of the United Nations' GEF international mangrove demonstration zones.

4.3. Mangrove Accretion Response to the Relative SLR

The vulnerability of mangroves to SLR depends on the magnitude of their accretion and subsidence rates and their elevation capital, as noted by Semeniuk (1994) and Lovelock et al. (2015) [19,60]. Mangroves at the interface of terrestrial and marine ecosystems are particularly sensitive to environmental change [27]. SLR is a significant driving force for the landward migration of mangroves, and mangroves may be able to counteract regional SLR at the case site. It remains to be fully clarified whether, under greenhouse gas emission scenarios, mangrove vertical soil accretion can sufficiently counteract SLR rate in the future.

4.3.1. Response of Mangroves in Beilun Estuary to Relative SLR

Based on stochastic dynamic modeling [61] incorporating climate-driven variables and long-term historical tide gauge records from Fangchenggang marine station from 1996 to 2024 (Figure 4), we estimated the projected SLR. The model formulates the mean sea level sequence as follows:

$$Y(t) = T(t) + P(t) + X(t) + \alpha(t) \quad (1)$$

where $Y(t)$ denotes the monthly average sea level; $T(t)$ represents the deterministic trend term; $P(t)$ is the deterministic periodic term; $X(t)$ signifies the residual random sequence; $\alpha(t)$ is the white noise sequence; and t denotes time.

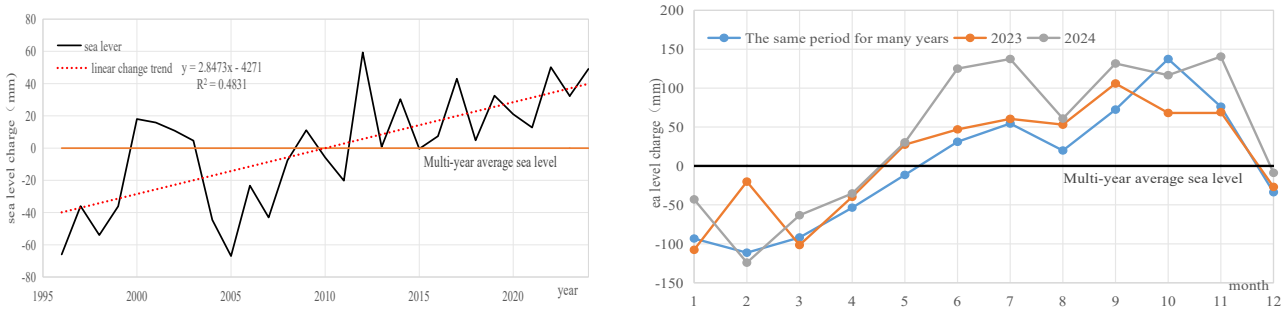

(**a**) Sea level change from 1996 to 2024.

(**b**) Monthly mean sea level change.

Figure 4. Sea level change from 1996 to 2024 and monthly mean sea level change in Fangchenggang city near Beilun estuary.

The deterministic trend term is expressed as a polynomial:

$$T(t) = A_0 + Bt \quad (2)$$

Here, A_0 is the mean sea level in the starting month, and B represents the linear sea level change rate.

Assuming K significant periodic components exist in the sea level series, the deterministic periodic term is defined as follows:

$$P(t) = \sum_{i=1}^{K} C_i cos(\sigma_i t - \varphi_{i0}) \quad (3)$$

where, σ_i is the angular frequency, and C_i and φ_{i0} denote the amplitude and initial phase angle of the i-th periodic component, respectively.

The linear least squares method was employed to fit and compute the trend coefficients (A_0, B) and periodic term coefficients of the deterministic component. Once the deterministic part (C_i and φ_{i0}) was derived, it was subtracted from the original data to obtain the residual sequence:

$$\mathrm{Y}'(\mathrm{t}) = Y(t) - \left\{ A_0 + Bt + \sum_{i=1}^{K} C_i cos(\sigma_i t - \varphi_{i0}) \right\} \quad (4)$$

This residual sequence can be treated as a random process due to the removal of deterministic components. Upon testing, if the residual sequence is found to be stationary, normally distributed, and non-independent, a stochastic dynamic autoregressive (AR) model is established for the residuals $\mathrm{Y}'(\mathrm{t})$:

$$\mathrm{Y}'(\mathrm{t}) = \sum_{\mathrm{j}=1}^{\mathrm{p}} \varnothing_{\mathrm{j}} \mathrm{Y}'(\mathrm{t}-\mathrm{j}) \quad (5)$$

where $\varnothing_{\mathrm{j}}$ is an autoregressive coefficient and p is the order of the autoregressive model.

The model order P is determined by the minimum information criterion, expressed as

$$AIC = Nlog_e\sigma_a^2 + 2(P+1) \quad (6)$$

where P is selected to minimize

$$\begin{cases} \sigma_a^2 = r(0) - \sum_{j=1}^{p} \varnothing_j r(j) \\ S^2 = \frac{1}{N} \sum_{t=1}^{N} Y'(t)^2 \\ r(m) = \frac{1}{N-1} \sum_{t=1}^{N-m} \left[\frac{Y'(t)Y'(t+m)}{S^2} \right], (m = 0, 1, P) \end{cases} \quad (7)$$

where S^2 is the mean of the residual sum of squares, represents the residual autocovariance function, and denotes the white noise variance.

The autoregressive coefficients are calculated using the following recursive Formula (8):

$$\begin{cases} \varnothing_1^1 = \frac{r(1)}{r(0)} \\ \varnothing_P^P = \frac{r(P) - \sum_{J=1}^{P-1} \varnothing_j^{p-1} r(j)}{r(0) - \sum_{J=1}^{P-1} \varnothing_j^{p-1} r(j)} \\ \varnothing_j^P = \varnothing_j^{P-1} - \varnothing_p^P \varnothing_{P-j}^{P-1}, (j = 1, 2, ..., P-1) \end{cases} \quad (8)$$

By superimposing the deterministic component with the stochastic dynamic model, a comprehensive SLR analysis and prediction model is formed:

$$Y(t) = A_0 + Bt + \sum_{i=1}^{K} C_i cos(\sigma_i t - \varphi_{i0}) + \sum_{\mathrm{j}=1}^{\mathrm{p}} \varnothing_{\mathrm{j}} \mathrm{Y}'(\mathrm{t}-\mathrm{j}) + \mathrm{a}(\mathrm{t}) \quad (9)$$

The results show that the sea-level rise (SLR) rate in the Beilun estuary is 2.8 mm/a (Figure 4a), which is lower than the multi-year mean SLR rate along China's coasts (3.5 mm/a) [62] but higher than that along the Guangxi coasts (2.1 mm/a according to the long-term observation data of the Beihai marine station) [63]. In 2024, the sea level along the coast of the Beilun estuary was 49 mm above the multi-year average sea level and 17 mm higher than in 2023. The sea level changes in each month fluctuated greatly along the Beilun estuary (Figure 4b). In 2024, the sea level was lower in February and October than in the same periods in many previous years. The sea level in November was 64 mm higher than it was in the same period for many years.

At present, based on the results of this study and prior publications, the mangrove vertical soil accretion, 0 ± 1.95 mm/a (range: 1.10–10.54 mm/a, n = 10), is higher than SLR rate (2.8 mm/a) along the Beilun estuary. The mangroves in the Beilun estuary are able to resist the current SLR. However, some stations (ZZW-1 and ZZW-2) in the Pear Bay

mangrove wetland must be protected and restored to resist the risk of seawater inundation. Based on model projections, the sea level along the Beilun estuary is estimated to rise by 70–142 mm by 2050 (at an mean annual SLR rate of 2.69–5.46 mm/a) and by 210–426 by 2100 (at an mean annual SLR rate of 2.76–5.61 mm/a), reflecting multi-decadal variability under projected climate scenarios. These ranges reflect the uncertainty in long-term projections, which may be influenced by climate change, ocean dynamics, and other factors.

Under low-emissions scenarios, if the sediment sources and input of vertical soil accretion remain stable, by the end of 2050 (mean annual rate of 2.69 mm/a) and 2100 (mean annual rate of 2.76 mm/a), approximately 80% of the surveyed mangrove stations (station ratio = 2/10) across the Beilun estuary may be able to withstand SLR except for some stations in Pear Bay (ZZW-1 and ZZW-2), which will experience flooding. Under high-emissions scenarios, by the end of 2050 (mean annual rate of 5.46 mm/a) and 2100 (mean annual rate of 5.61 mm/a), approximately 60% of the surveyed stations (station ratio = 6/10) will experience flooding, including in Pear Bay (SJ-1, ZZW-1, ZZW-2, and ZZW-3) and Yuzhouping (YZP-1 and YZP-2).

4.3.2. Response of Mangroves in Guangxi Coastal Zone to Relative SLR

The SLR rate the Guangxi coastal zone, as reported by Huang et al. (2021) [64], has shown a gradual increase since 1965 at a rate of 2.5 mm/a from 1980 to 2019, reaching historically high levels since 2001. In the Beibu Gulf, the sea level in 2011–2019 was approximately 46 mm higher than the sea level in 2001–2010, about 94 mm higher than the sea level during in 1981–1990, and roughly 68 mm higher than of the sea level in 1991-2000 [64]. Our study analyzes sea level changes along the Guangxi coastal zone by applying the aforementioned stochastic dynamic model to long-term observation data from the Beihai marine station from 1996 to 2024 (Figure 5). Our results show that SLR rate along the Guangxi coastal zone is 2.1 mm/year from 1966 to 2024 (Figure 5a), which is lower than the multi-year mean SLR along Chinese coasts (3.5 mm/a) [62]. In 2024, the sea level along the coast of Guangxi was 65 mm higher than the multi-year average sea level and 13 mm higher than the level in 2023 (Figure 5a). Along the Guangxi coastal zone, the sea level changes in each month fluctuated greatly (Figure 5b). In 2024, the sea level was lower in February and October than it had been for many years, and the sea level in November was 68 mm higher than it had been in the same period for many years. Based on projections for the Guangxi coastal zone, the sea level is anticipated to rise by 51 to 130 mm by 2050 (at a mean annual SLR rate of 1.96–5.00 mm/a). Looking further ahead to 2100, the projected sea level rise in this area is expected to range from 135 to 387 mm (at a mean annual SLR rate of 2.04–5.09 mm/a).

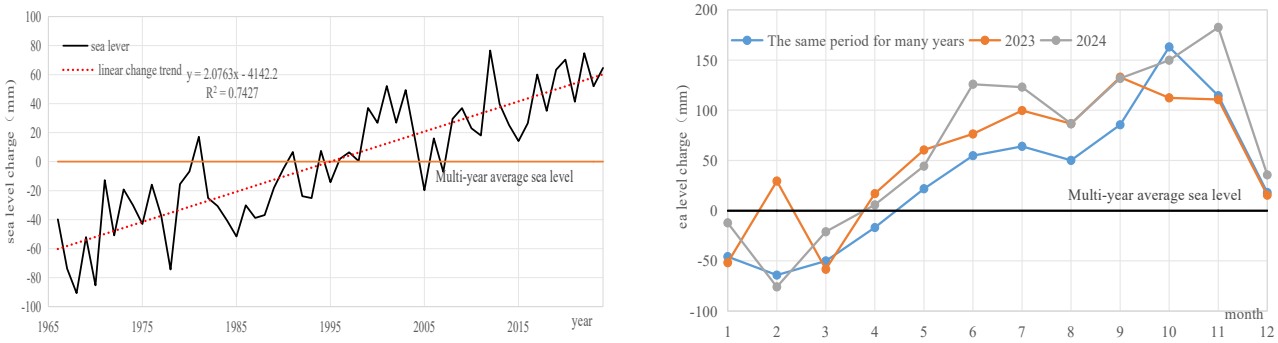

(**a**) Annual mean sea level change. (**b**) Monthly mean sea level change.

Figure 5. Annual and monthly mean sea level fluctuations in Guangxi coastal zone between 1996 and 2024.

Based on the above comprehensive analysis, we have forecasted SLR rates across the entire Guangxi coastal zone in 2050 and 2100 using long-term observation data from the Fangchenggang Marine Station and Beihai Marine Station. By the end of 2050 AD, the mean annual SLR rate is anticipated to 2.33 mm/a (from 1.96 to 2.69 mm/a) under low-emissions scenarios and 5.23 mm/a (from 5.00 to 5.46 mm/a) under low-emissions scenarios. By the end of 2100, the mean annual SLR rate is anticipated to be 2.40 mm/a (from 2.04 to 2.76 mm/a) under low-emissions scenarios and 5.35 mm/a (from 5.09 to 5.61 mm/a) under low-emissions scenarios. If the sediment sources and input of vertical soil accretion remain stable, under low-emissions scenarios, by the end of 2050 (the mean annual rate of 2.33 mm/a) and 2100 (mean annual rate of 2.40 mm/a), approximately 1.6% (station ratio = 6/37) of the surveyed stations will experience flooding, including Pear Bay (ZZW-1 and ZZW-2), Tieshangang (Tieshan port TSW-1), Dandouhai (DDH), Yingluo bay (YLW02 and YLW04). Under high-emissions scenarios, by the end of 2050 (the mean annual rate of 5.23 mm/a) and 2100 (the mean annual rate of 5.35 mm/a), approximately 43% of the surveyed stations (station ratio = 16/37) will experience flooding, including Pear Bay (SJ-1, ZZW-1, ZZW-2, and ZZW-3), Yuzhouping (Dong Bay, YZP-1, and, YZP-2), Maoweihai-Qinjiang estuary (JXW), Jinhai Bay (Daguansha, Z1, DGS1-2, and JHW1), Tieshangang (Tieshan port TSW-1), Dandouhai (DDH), Yingluo bay (O18, YLW01, YLW02, YLW03, and YLW04) (see Figure 3 and Table S6).

4.4. Countermeasures to the Mitigate Mangrove Accretion Response to the Relative SLR

The cumulative impact of the relative SLR will exacerbate coastal erosion and the severity of storm surges along the Guangxi coasts in the future. Under high-emissions scenarios, by the end of 2050 and 2100, the mangrove wetlands along the Guangxi coastal zone will be unable to withstand SLR, including mangroves in Pear Bay, Yuzhouping, the Maoweihai–Qinjiang estuary, Jinhai Bay (Daguansha), Tieshangang (Tieshan port), Dandouhai, and Yingluo bay. To address the risks of SLR, it is necessary to increase coastal protection to enhance ecological adaptability to the relative SLR. Thus, the following measures are recommended:

First and foremost, it is crucial to increase monitoring of vertical soil accretion and elevation changes in coastal wetlands. This should be a long-term and ongoing effort using various methods, including radiometric, SET-MH, and event horizon approaches. Additionally, enhancing and optimizing refined prediction models for sea-level rise is critical to accurately understand its rhythm and trend. A comprehensive scientific system for assessing sea levels should be established to promote risk analysis of SLR under various scenarios, including coastal bodies that can withstand major disasters, coastal city safety, typical coastal ecosystems, water resources, and spatial patterns of land.

Second, it is essential to give due consideration to the seasonal high sea-level period that occurs annually from September to November in the Guangxi coastal zone. This period accounts for nearly two-thirds of the catastrophic storm surge disasters that took place during the past decade, specifically when seasonal high sea levels, astronomical spring tides, and storm surges converged. Effective measures should be implemented to establish a sustainable coastal protection system, for instance, mangrove in-situ ecological conservation and ecological coast construction [65–67].

Numerous “hard” structures such as coastal levees, seawalls, and breakwaters have been constructed to safeguard the coastal zone, despite the fact that they entail significant maintenance expenses and can harm the ecosystem. A novel environmentally friendly “green” coastal concept is introduced for safeguarding the coasts, which is grounded in a three-dimension model (also referred to as three factors, specifically the longitudinal, lateral, and vertical dimensions) and taking into account moisture resistance measures [65–69].

The ecological coast harnesses the full potential of coastal vegetation's protective function against natural disasters, like storm surges and coastal erosion, while simultaneously addressing landscape greening and biodiversity conservation needs. Compared to conventional "hard" coastal structures, the ecological coast attenuates and prevents waves, reduces pollution, and provides habitats while also playing a crucial role in carbon sequestration and carbon sink enhancement. In fact, to mitigate the impact of SLR, a "green" ecological coast model was proposed in 2017 and is being piloted in regions of China, including Guangdong, Guangxi, and Shanghai [65].

5. Conclusions

In the context of global warming and increasing extreme weather events, the question of whether mangroves can adapt to SLR is of paramount importance. Protecting and restoring coastal wetlands to further maintain or increase vertical soil accretion, enhance the resilience of ecological functions, and improve the sustainable capacity to withstand marine disasters has emerged as a key focus. Our results demonstrate that soil elevation in the Beilun estuary mangroves is increasing through biotic controls and can keep up with SLR at present. However, with ongoing coastal development, urban expansion, and human interference, it is uncertain if vertical soil accretion will continue to be able to effectively counteract SLR by the end of 2100. Our findings provide critical insights into mangrove adaptive capacity under projected SLR scenarios, underscoring the need for integrated management strategies that balance sediment supply maintenance and ecological restoration to ensure long-term resilience. The Guangxi coastal zone is vulnerable to destructive tropical cyclones and astronomical spring tides, which can exacerbate the impact of seasonal high sea levels and storm surges, leading to increased disaster risk. In order to improve ecological adaptability for coastal protection, the implementation of "green" ecological coasts in lieu of traditional "hard" coastal facilities should be prioritized.

Supplementary Materials: The following supporting information can be downloaded at: https://www.mdpi.com/article/10.3390/su17188099/s1, Tables S1–S6 and Figure S1 [27,41,50–55,70].

Author Contributions: P.Z.: Conceptualization, sampling and data processing, methodology, and writing—review and editing. J.Z. and D.L.: Analysis, data processing, and writing. J.Z. and Z.J.: writing—review and editing. All authors have read and agreed to the published version of the manuscript.

Funding: This research was funded by Science and Technology Development Foundation of South China Sea Bureau, Ministry of Natural Resources of P. R. China (240104 and 23YD03), and the Fund of Key Laboratory of Global Change and Marine-Atmospheric Chemistry (GCMAC) of Ministry of Natural Resources (MNR) of P. R. China (GCMAC202207).

Institutional Review Board Statement: Not applicable.

Informed Consent Statement: Not applicable.

Data Availability Statement: The data presented in this study are available in insert article here.

Acknowledgments: We are grateful for the sampling help from Beihai Marine Center Station of Ministry of Natural Resources of P. R. China (Guiwen Zhu and Guoqing Liu), Fangchenggang Ocean Bureau (Wanci Luo and Xiong Lliu), and Guangxi Beilun Estuary National Nature Reserve Administration (Zhihe Wu) of Guangxi Zhuang Autonomous Region. Finally, we are extremely thankful for Jianghai Wang (School of Marine Science, Sun Yat-sen University) for revisiting the overall storyline and the English language in the paper.

Conflicts of Interest: The authors declare no conflicts of interest.

References

1. Kirwan, M.L.; Megonigal, J.P. Tidal wetland stability in the face of human impacts and sea-level rise. *Nature* **2013**, *504*, 53–60. [CrossRef]
2. Murray, B.C. Mangroves' hidden value. *Nat. Clim. Change* **2012**, *2*, 773–7747. [CrossRef]
3. Nagelkerken, I.; Blaber, S.J.M.; Bouillon, S.; Green, P.; Haywood, M.; Kirton, L.G.; Meynecke, J.-O.; Pawlik, J.; Penrose, H.M.; Sasekumar, A.; et al. The habitat function of mangroves for terrestrial and marine fauna: A review. *Aquat. Bot.* **2008**, *89*, 155–185. [CrossRef]
4. Guannel, G.; Arkema, K.; Ruggiero, P.; Verutes, G. The power of three: Coral reefs, seagrasses and mangroves protect coastal regions and increase their resilience. *PLoS ONE* **2016**, *11*, e0158094. [CrossRef]
5. Zhang, Y.; Zhang, Z.; Meng, H.; Zhang, L.; Yu, K. Geochemical evidences of the land subsidence induced by the historical earth quake in 1605, Hainan Island, China. *Quat. Sci.* **2012**, *32*, 1248–1254. (In Chinese with English Abstract). [CrossRef]
6. Kirwan, M.L.; Temmerman, S.; Skeehan, E.E.; Guntenspergen, G.R.; Fagherazzi, S. Overestimation of marsh vulnerability to sea level rise. *Nat. Clim. Change* **2016**, *6*, 253–260. [CrossRef]
7. Duan, S.; Xu, J. Functions of mangrove wetlands in the conservation of the coastal ecosystems. *Ecol. Sci.* **2004**, *23*, 351–355. (In Chinese with English Abstract)
8. Huang, Q. Evaluation on the Value of Mangrove Ecosystem Services at Beilun Estuary of Guangxi. Master's Thesis, Guangxi Normal University, Guilin, China, 2018; pp. 1–60. (In Chinese with English Abstract)
9. Rovai, A.S.; Twilley, R.R.; Castañeda-Moya, E.; Riul, P.; Cifuentes-Jara, M.; Manrow-Villalobos, M.; Horta, P.A.; Simonassi, J.C.; Fonseca, A.L.; Pagliosa, P.R. Controls on carbon storage in mangrove soils. *Nat. Clim. Change* **2018**, *8*, 534–538. [CrossRef]
10. Yessoufou, K.; Stoffberg, G.H. Biogeography, threats and phylogenetic structure of mangrove forest globally and in South Africa: A review. *South Afr. J. Bot.* **2016**, *107*, 114–120. [CrossRef]
11. Zhang, Q.; Sui, S. The Mangrove wetland resources and their conservation in China. *J. Nat. Resour.* **2001**, *16*, 28–36. (In Chinese with English Abstract)
12. WMO (World Meteorological Organization, UN). *WMO Greenhouse Gas Bulletin- No.16: The State of Greenhouse Gases in the Atmosphere Based on Global Observations Through 2019*; WMO: Geneva, Switzerland, 2020.
13. Nicholls, R.J.; Wong, P.P.; Burkett, V.; Codignotto, J.; Woodroffe, C.D. *Coastal systems and low-lying areas//Climate Change 2007: Impacts, Adaptation and Vulnerability*; Cambridge University Press: Cambridge, UK, 2007; pp. 124–129.
14. Watson, R.T.; Zinyowera, M.C.; Moss, R.H. *Climate Change 1995: Impacts, Adaptations and Mitigation of Climate Change, Scientific Technical Analysis*; Cambridge University Press: Cambridge, UK, 1996.
15. MNR (Ministry of Natural Resources, P.R. China). China Sea Level Bulletin in 2020. 26 April 2021. Index No. 000019174/2021–00211. (In Chinese). Available online: https://gi.mnr.gov.cn/202104/t20210426_2630186.html (accessed on 3 September 2025).
16. Kopp, R.E.; Horton, R.M.; Little, C.M.; Mitrovica, J.X.; Oppenheimer, M.; Rasmussen, D.J.; Strauss, B.H.; Tebaldi, C. Probabilistic 21st and 22nd century sea-level projections at a global network of tide-gauge sites. *Earths Future* **2014**, *2*, 383–406. [CrossRef]
17. Saintilan, N.; Khan, N.S.; Ashe, E.; Kelleway, J.J.; Rogers, K.; Woodroffe, C.D.; Horton, B.P. Thresholds of mangrove survival under rapid sea level rise. *Science* **2020**, *368*, 1118–1121. [CrossRef] [PubMed]
18. Valiela, I.; Bowen, J.L.; York, J.K. Mangrove forests: One of the world's threatened major tropical environments. *BioScience* **2001**, *51*, 807–815. [CrossRef]
19. Lovelock, C.E.; Cahoon, D.R.; Friess, D.A.; Guntenspergen, G.R.; Krauss, K.W.; Reef, R.; Rogers, K.; Saunders, M.L.; Sidik, F.; Swales, A.; et al. The vulnerability of Indo-Pacific mangrove forests to sea-level rise. *Nature* **2015**, *526*, 559–563. [CrossRef] [PubMed]
20. Coldren, G.A.; Langley, J.A.; Feller, I.C.; Chapman, S.K. Warming accelerates mangrove expansion and surface elevation gain in a subtropical wetland. *J. Ecol.* **2018**, *107*, 79–90. [CrossRef]
21. Ball, M.C. Ecophysiology of mangroves. *Trees-Struct. Funct.* **1988**, *2*, 129–142. [CrossRef]
22. Woodroffe, C.D. The impact of sea-level rise on mangrove shorelines. *Prog. Phys. Geogr.* **1990**, *14*, 483–520. [CrossRef]
23. Woodroffe, C.D. Response of tide-dominated mangrove shorelines in Northern Australia to anticipated sea-level rise. *Earth Surf. Process. Landf.* **1995**, *20*, 65–85. [CrossRef]
24. Woodroffe, C.D. *Coasts: Form, Process, and Evolution*; Cambridge University Press: Cambridge, UK, 2002.
25. Woodroffe, C.D.; Rogers, K.; McKee, K.L.; Lovelock, C.E.; Mendelssohn, I.A.; Saintilan, N. Mangrove sedimentation and response to relative sea-level rise. *Ann. Rev. Mar. Sci.* **2016**, *8*, 243–266. [CrossRef]
26. Krauss, K.W.; McKee, K.L.; Lovelock, C.E.; Cahoon, D.R.; Saintilan, N.; Reef, R.; Chen, L. How mangrove forests adjust to rising sea level. *New Phytol.* **2014**, *202*, 19–34. [CrossRef]
27. Xia, P.; Meng, X.; Feng, A.; Li, Z.; Yang, G. Sediment compaction rates in mangrove swamps of Guangxi and its mangrove migration response to sea-level rise. *Acta Sedimentol. Sin.* **2015**, *33*, 551–560. (In Chinese with English Abstract). [CrossRef]
28. Yang, Y. Evaluating the Spatial Vulnerability of Mangroves from Reclamation in Mainland China's Coastal Area. Master's Thesis, Xiamen University, Xiamen, China, 2018; pp. 9–19. (In Chinese with English Abstract)

29. Fan, H.; Mo, Z. The history, achievements and lessons learned for mangrove restoration in Guangxi, China. *Guangxi Sci.* **2018**, *25*, 363–371+387. (In Chinese with English Abstract). [CrossRef]
30. Hu, G.; Li, J.; Qin, Y.; Hu, B.; Liu, X.; Zhang, Z. Population structure and dynamics of mangrove species in Beilun Estuary, Guangxi, southern China. *Acta Ecol. Sin.* **2018**, *38*, 3022–3034. (In Chinese with English Abstract). [CrossRef]
31. Xiong, X.; Wang, X.; Zhou, H.; Wu, P. The distribution of mangrove bacteria in intertidal surface sediments of the Beilun Estuary. *Mar. Environ. Sci.* **2008**, *3*, 101–106. (In Chinese with English Abstract). [CrossRef]
32. Dan, X.; Liao, B.; Wu, Z.; Wu, H.; Bao, D.; Dan, W.; Liu, S. Resources, protection status and major threats of Chinese mangrove wetland. *Ecol. Environ. Sci.* **2016**, *25*, 1237–1243. (In Chinese with English Abstract). [CrossRef]
33. Li, D.; Zhao, L.; Guo, Z.; Yang, X.; Deng, W.; Zhong, H.; Zhou, P. Marine debris in the Beilun Estuary mangrove forest: Monitoring, assessment and implications. *Int. J. Environ. Res. Public Health* **2021**, *18*, 10826. [CrossRef]
34. He, X.; Su, B.; Xu, T.; Nong, L.; Ye, C.; Li, X. Macrobenthic biodiversity in mangrove wetland at the estuary of Beilun River in Guangxi. *Wetl. Ecol. Manag.* **2012**, *8*, 45–48. (In Chinese with English Abstract). [CrossRef]
35. Lai, J.; Xu, M.; Jiang, F.; Ke, K.; Zhang, R.; Lei, F. Marine ecosystem environmental health assessment in the coastal waters of Beilun Estuary. *Guangxi Sci.* **2014**, *21*, 77–83. (In Chinese with English Abstract). [CrossRef]
36. Liu, X.; Cheng, D.; Ye, C.; Su, B.; Luo, W.; Zeng, X.; Xu, L.; Luo, Z. Changes of water quality parameters along the coastal area of National Nature Reserve of Guangxi Beilun Estuary, 2012–2014. *J. Guangxi Acad. Sci.* **2015**, *31*, 89–93. (In Chinese with English Abstract). [CrossRef]
37. Li, B.; Pang, B.; Tan, Q.; Wu, L. Distribution, influence and risk assessment of polycyclic aromatic hydrocarbons (PAHs) in the mangrove underground in situ pipe eco-farming system in Beilun Estuary. *Mar. Fish.* **2019**, *41*, 520–535. (In Chinese with English Abstract)
38. Gong, Y. Analysis on the Ecological Changes and Protection of Mangroves in the Beilun Estuary Jings' Residence. Master's Thesis, Guangxi University for Nationalities, Guilin, China, 2019; pp. 1–93. (In Chinese with English Abstract)
39. Zhu, J.; Zhang, Q.; Li, Y.; Tan, S.; Kang, Z.; Yu, X.; Lan, W.; Cai, L.; Wang, J.; Shi, H. Microplastic pollution in the Maowei Sea, a typical mariculture bay of China. *Sci. Total Environ.* **2019**, *658*, 62–68. [CrossRef] [PubMed]
40. Zhou, Q.; Tu, C.; Fu, C.; Li, Y.; Zhang, H.; Xiong, K.; Zhao, X.; Li, L.; Waniek, J.J.; Luo, Y. Characteristics and distribution of microplastics in the coastal mangrove sediments of China. *Sci. Total Environ.* **2020**, *703*, 134807. [CrossRef]
41. Liu, T.; Chu, G.; Xu, H. Using storm deposition in mangrove for dating and sedimentary dynamic analysis. *Acta Sedimentologica Sinica.* **2022**. (In Chinese with English Abstract). [CrossRef]
42. Liu, G.; Chen, M.; Huang, Y.; Li, Y. Measurement of radionuclides in sediments core by HPGe γ spectroscopy. *J. Xiamen Univ. (Nat. Sci.)* **2001**, *40*, 669–674. (In Chinese with English Abstract)
43. Li, D.; Xu, M.; Liu, G.; Li, C. Distribution of radioisotopes in sediment cores from nearshore off Xinghua Bay mouth, Fujian, China. *J. Radioanal. Nucl. Chem.* **2007**, *273*, 151–155. [CrossRef]
44. Zhou, P.; Li, D.; Li, H.; Fang, H.; Huang, C.; Zhang, Y.; Zhang, H.; Zhao, L.; Zhou, J.; Wang, H.; et al. Distribution of radionuclides in a marine sediment core off the waterspout of the nuclear power plants in Daya Bay, northeastern South China Sea. *J. Radioanal. Nucl. Chem.* **2015**, *145*, 102–112. [CrossRef]
45. *GB/T 30738-2014*; Determination of Radionuclide in Marine Sediment—Gamma Spectrometry. China National Standardization Administration: Beijing, China, 2014.
46. Goldberg, E.D. "Geochronology with ^{210}Pb, in radioactive dating" in Radioactive Dating. In Proceedings of the symposium on Radioactive Dating, Athens, Greece, 19–23 November 1962; pp. 21–131.
47. Oldfield, F.; Appleby, P.G.; Thompson, R. Paleoecological studies of lakes in the highlands of Papua New Guinea. *J. Ecol.* **1980**, *68*, 457–477. [CrossRef]
48. Cochran, J.K. The fates of uranium and thorium decay series nuclides in the estuarine environment. In *The Estuary as a Filter*; Kennedy, V.S., Ed.; Academic Press: Cambridge, MA, USA, 1984; pp. 179–220.
49. Li, Y.; Bergen, G.W.; ven Weering, T.C.E. ^{210}Pb as a tracer for the tidal fiat sedimentation in the southern Hangzhou Bay. *Donghai Mar. Sci.* **1993**, *11*, 34–43. (In Chinese with English Abstract)
50. Chu, G. Study on Sedimentation and Carbon Burial Characteristics and Vulnerability of Mangroves Based on Storm Surge History in Guangxi. Master's Thesis, Guangxi University, Nanning, China, 2022; pp. 1–58. (In Chinese with English Abstract)
51. Liu, T.; Liu, Y.; Yu, Y. Response of mangrove swamp sedimentation rate to climate change. *J. Trop. Oceanogr.* **2017**, *36*, 40–47. (In Chinese with English Abstract)
52. Luo, Z.; Meng, X.; Luo, X. Impact of global sea level rise, crustal rise and tidal flat sedimentation for one hundred years on the mangrove distribution in the Yingluo Bay of Guangxi. *Mar. Sci. Bull.* **2017**, *36*, 209–216. (In Chinese with English Abstract). [CrossRef]
53. Xu, H. Study on Sedimentary and Carbon Burial Characteristics and Expansion History of Typical Mangroves in Guangxi. Master's Thesis, Guangxi University, Nanning, China, 2020; pp. 1–73. (In Chinese with English Abstract)

54. Li, Z. Palynological Assemblage and Environment Evolution of the Coastal Zone Within the Last Hundred Years in Guangxi. Master's Thesis, East China Normal University, Shanghai, China, 2010. (In Chinese with English Abstract)
55. Li, Z.; Li, J.; Zhang, W.; Li, Z.; Li, C.; Liu, L.; Meng, X. Pollen assemblage and sedimentary environment evolution in the coastal zone in Qinzhou Bay, Guangxi province. *Quat. Sci.* **2010**, *30*, 558–608. (In Chinese with English Abstract).
56. Alongi, D.M.; Pfitzner, J.; Trott, L.A.; Tirendi, F.; Dixon, P.; Klumpp, D.W. Rapid sediment accumulation and microbial mineralization in forests of the mangrove Kandelia candel in the Jiulongjiang Estuary, China. *Estuar. Coast. Shelf Sci.* **2005**, *63*, 605–618. [CrossRef]
57. Gao, Y.; Yuan, D.; Lu, B.; Sun, L.; Lin, H.; Huang, S. Spacio temporal distribution of mercury in core sediments of the mangrove ecosystem in Jiulongjiang Estuary. *J. Appl. Oceanogr.* **2016**, *35*, 58–64. (In Chinese with English Abstract). [CrossRef]
58. Breithaupt, J.L.; Smoak, J.M.; Bane, R.H.; Waters, M.N.; Moyer, R.P.; Sanders, C.J. Avoiding timescale bias in assessments of coastal wetland vertical change. *Limnol. Oceanogr.* **2018**, *63*, S477–S495. [CrossRef] [PubMed]
59. Fan, H.; Wang, X.; He, B.; Pan, L. *Artificial Habitat Establishment and Mangrove Rehabilitation*; Forestry Press: Beijing, China, 2014. (In Chinese)
60. Semeniuk, V. Predicting the effect of sea level rise on mangroves in northwestern Australia. *J. Coast. Res.* **1994**, *10*, 1050–1076.
61. Tian, H.; Zhou, T.; Chen, Z. A stochastic dynamical prediction model of mean sea level changes. *J. Ocean Uuniversity Qingdao* **1993**, *23*, 33–42. (In Chinese with English Abstract)
62. MNR (Ministry of Natural Resources, China). China Sea Level Bulletin in 2023. 15 April 2024. Index No. 000019174/2024-00002. (In Chinese). Available online: https://gi.mnr.gov.cn/202404/t20240429_2844012.html (accessed on 3 September 2025).
63. Marine Bureau of Guangxi Zhuang Autonomous Region. Marine Disasters and Sea Level Bulletin of Guangxi Zhuang Autonomous Region in 2023. June 2024. (In Chinese). Available online: http://hyj.gxzf.gov.cn/zwgk_66846/hygb_66897/hyzhgb/t18529082.shtml (accessed on 3 September 2025).
64. Huang, X.; Chen, Y.; Mo, W.; Fan, H.; Liu, W.; Sun, M.; Xie, M.; Xu, S. Climate change and its influence in Beibu Gulf mangrove biome of Guangxi in past 60 years. *Acta Ecol. Sin.* **2021**, *41*, 5026–5033. (In Chinese with English Abstract). [CrossRef]
65. SOA (State Oceanic Administration, China). China Sea Level Bulletin in 2017. 23 April 2018. (In Chinese). Available online: https://gc.mnr.gov.cn/201806/t20180619_1798298.html (accessed on 3 September 2025).
66. Zhang, H.; Han, G.; Wang, D.; Xue, Q.; Luo, Y. Ecological engineering based adaptive coastal defense strategy to global change. *Adv. Earth Sci.* **2015**, *30*, 996–1005. (In Chinese with English Abstract)
67. Wang, H. The Coastal Protection Based on Ecological Concept. China Natural Resources News. (In Chinese). Available online: https://scs.mnr.gov.cn/scsb/shyw/202105/6d3b2a328b744d9984d03f63991735b7.shtml (accessed on 13 May 2021).
68. Yang, Z.; Zhang, Z.; Suo, A.; Wen, Q. Discussion on coastal zone protection and utilization planning based on the concept of "Ecological priority". In Proceedings of the CSES (Chinese Society of Environmental Science) Annual Conference of Science and Technology in 2018 (Vol. I), Hefei, China, 3–5 August 2018. (In Chinese with English Abstract)
69. Xu, W.; Tao, A.; Liu, J.; Chen, C.; Yu, F.; Zhang, Z. The enlightenment of international coastal zone ecological protection for China's ecological sea dike construction. *Ocean. Dev. Manag.* **2019**, *36*, 12–15. (In Chinese with English Abstract)
70. Zhang, Q.; Wen, X.; Song, C.; Liu, S. The measurement and study on sedimentation rates in mangrove tidal flats. *Trop. Oceanol.* **1996**, *15*, 57–62. (In Chinese with English Abstract)

Disclaimer/Publisher's Note: The statements, opinions and data contained in all publications are solely those of the individual author(s) and contributor(s) and not of MDPI and/or the editor(s). MDPI and/or the editor(s) disclaim responsibility for any injury to people or property resulting from any ideas, methods, instructions or products referred to in the content.